

# What Can Be Learned by Measuring the Fluxes of the ${}^7\text{Be}$ and the *pep* Solar Neutrino Lines ?

J.N. Bahcall and P.I. Krastev

*School of Natural Sciences, Institute for Advanced Study*

*Princeton, NJ 08540*

## Abstract

Measurements of the interaction rates of the solar neutrino lines of  ${}^7\text{Be}$  and *pep* can be used, independent of solar models, to test whether electron flavor is conserved, to determine survival probabilities of electron-type neutrinos at specific energies, and to test for the existence of sterile neutrinos. We present analytic descriptions of these tests. We also illustrate by numerical simulations, assuming matter-enhanced and vacuum neutrino oscillations, what measurements of solar neutrino lines can teach us about neutrino masses and mixing angles.

PACS number(s): 26.65.+t, 14.60.Pq, 13.15.+g, 23.40.Bw, 96.60.-j

## I. INTRODUCTION

Figure 1 shows the electron recoil spectrum that we calculate for neutrino-electron scattering. Although, as Figure 1 makes clear, the sun is predicted to produce important sources of low-energy neutrinos with energies of order an MeV or less, there are no operating detectors that can measure individual neutrino energies in this low energy range. In particular, there is currently no way to isolate experimentally the fluxes of the predicted strong solar neutrino lines.

We urge readers who are familiar with solar neutrino research to turn immediately to Section VII, which contains a concise summary and discussion of our analysis of what can be learned about neutrino properties from studying solar neutrino lines. We do not discuss here what can be learned about the solar interior from studying neutrino lines<sup>1</sup>.

Continuum neutrino sources, principally neutrinos from  $^8\text{B}$  decay and from the  $pp$  reaction, are believed to be the major contributors to the four pioneering solar neutrino experiments: chlorine [2], Kamiokande [3], GALLEX [4], and SAGE [5]. Moreover, the two next-generation experiments, Superkamiokande [6] and SNO [7], are both sensitive only to the neutrino continuum from  $^8\text{B}$  decay.

The four pioneering detectors have established experimentally that the sun shines by nuclear fusion reactions among light elements. Table I summarizes the results of these experiments.

Because the observed rates are lower than the predicted rates, the results from the operating experiments have led to a number of suggestions for new particle physics. In these particle physics scenarios, something causes a fraction of electron type neutrinos to disappear, or change their flavor, after they are created in the center of the sun. All of

---

<sup>1</sup>In ref [1], it is shown that a measurement of the energy shift of the  $^7\text{Be}$  solar neutrino line is equivalent to a measurement of the central temperature of the sun and a measurement of the energy profile of the  $^7\text{Be}$  line will determine the temperature profile of the solar interior.

the particle physics solutions of the solar neutrino problem predict a survival probability, the probability that an electron-type neutrino remains an electron-type neutrino, that is different from unity. In contrast, the survival probability is equal to unity in the simplest version of standard electroweak theory [8] .

Two new experiments, SNO and Superkamiokande, were designed with the goal in mind of establishing definitively if physics beyond the standard electroweak model is required to explain the results of solar neutrino experiments. Moreover, these new experiments will have the potential to determine the total flux (independent of flavor) of  ${}^8\text{B}$  solar neutrinos, thereby testing the prediction by solar models of the flux for this rare mode of neutrino production.

The most plausible particle physics explanations, resonant matter oscillations [9–11] (the Mikheyev-Smirnov-Wolfenstein, or MSW, effect) and vacuum neutrino oscillations [12], both predict a strong energy dependence for the survival probability. The form of the energy dependence is determined by the specific parameters used in the adopted oscillation scenario. Other suggested new particle physics explanations that predict a strong energy dependence for the survival probability include neutrino decay [13,14], non-standard electromagnetic properties [15–17], neutrino violation of the equivalence principle [18], and supersymmetric flavor-changing neutral currents [19,20]. Many of the relevant papers (and further references) are reprinted in [21].

We explore in this paper what can be learned about neutrino physics by performing experiments with solar neutrino lines.

Measurements with solar neutrino lines have the advantage that the predictions of particle physics models are more specific for a line source than they are for a continuum source. Measurements of continuum interaction rates determine a weighted average of what happens to neutrinos of different energies. Moreover, if a neutrino line is detected in two ways (e.g., by neutrino-electron scattering and by neutrino absorption) then the survival probability at a specific energy can be determined empirically, independent of any solar physics. At any energy, a measured value for the survival probability that is significantly different from unity

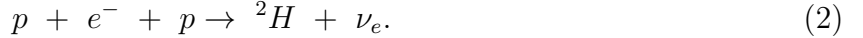
would constitute evidence for electron flavor non-conservation.

There are two nuclear reactions that are predicted to emit detectable numbers of solar neutrinos with specific energies, i.e., neutrino lines.<sup>2</sup> The more frequent of these reactions produces  ${}^7\text{Be}$  neutrinos via



Reaction (1) produces, according to the standard solar model [23,24], a total neutrino flux at earth of  $5 \times 10^9 \text{ cm}^{-2}\text{s}^{-1}$ , 89.7% of the neutrinos having, in the laboratory, an energy of  $E_\nu = 0.862 \text{ MeV}$  and the other 10.3% have  $E_\nu = 0.384 \text{ MeV}$ . The branching ratio of 9:1 is determined by nuclear physics and is the same in the laboratory and in the solar interior. The two  ${}^7\text{Be}$  lines can, in principle, be used to perform a unique test of the existence of sterile neutrinos (see Section VIB).

The *pep* neutrinos are created by the reaction



Reaction (2) produces neutrinos of energy  $E_\nu = 1.442 \text{ MeV}$ , with a standard solar model flux of  $1.4 \times 10^8 \text{ cm}^{-2}\text{s}^{-1}$ . In the standard solar model calculations, the total flux of  ${}^7\text{Be}$  neutrinos is about 35 times larger than the total flux of *pep* neutrinos. If neutrino oscillations occur, the predicted standard model ratio of  ${}^7\text{Be}$  to *pep* neutrino fluxes may be much reduced.

So far, BOREXINO [25], which will observe neutrino-electron scattering, is the only detector in an advanced stage of development that is being constructed with a goal of isolating events from a solar neutrino line. Two other experiments are being developed, HELLAZ [26] and HERON [27], which have the potential to detect solar neutrino lines via neutrino-electron scattering. Most recently, a Ga-As detector of low energy neutrinos has

---

<sup>2</sup>Although the fluxes from seven solar neutrino lines have been estimated [22], only the fluxes from the  ${}^7\text{Be}$  and the *pep* neutrino lines are expected to be large enough to be measurable in solar neutrino experiments that are currently feasible.

been proposed [28]. This detector could potentially measure the *pep* and the  ${}^7\text{Be}$  neutrino lines by neutrino-electron scattering and, very importantly, also by neutrino absorption (which would determine the charged current rate). For all of these experiments, good energy resolution will be required in order to separate the solar neutrino lines from continuum solar neutrino sources (cf. Figure 1) and from background events.

We begin, in Section II, by discussing neutrino-electron scattering experiments. We calculate the predicted electron recoil spectrum in neutrino-electron scattering experiments for four different neutrino oscillation scenarios and for the standard model (no oscillations, standard solar model). We then show to what extent measurements of the scattering rate for neutrino lines can be used to help determine neutrino masses and mixing angles. We calculate how much additional information can be gained by measuring both the  ${}^7\text{Be}$  and the *pep* neutrino lines, rather than concentrating (as originally planned in the BOREXINO experiment) on the  ${}^7\text{Be}$  line.

Next we demonstrate in Section III how survival probabilities at a specific energy can be measured if a neutrino line is studied both by a neutrino absorption experiment and by a neutrino-electron scattering experiment. We present a simple formula, Eq. (6), for the survival probability at the energy of the neutrino line; this formula is independent of all solar physics. We show in Section IV how neutral current experiments, when combined with either absorption or neutrino-electron scattering experiments can be used to determine the survival probability. In Section V, we focus on the model-independent inferences that are possible if both neutrino absorption and neutrino-electron scattering are measured. We show that, in a two-flavor scenario, the neutrino mixing angle and mass difference can be determined with reasonable accuracy if the absorption and neutrino-electron scattering rates are measured for both the  ${}^7\text{Be}$  and the *pep* lines. In Section VI, we show how studies of solar neutrino lines can help answer the question: Do sterile neutrinos exist? We summarize and discuss in Section VII the results obtained in this paper.

For the interested reader, we note that Bilenky and Giunti [29] have discussed, in a series of original and stimulating papers, the possibilities for using experiments that study the  ${}^8\text{B}$

continuum solar neutrinos to determine survival probabilities and to test for the existence of sterile neutrinos.

How can we assess what will be learned from different experiments without knowing which solution of the solar neutrino problem Nature has chosen? We must adopt some tentative model for how neutrinos behave in order to proceed. We assume successively the validity of either the small mixing angle (SMA) or the large mixing angle (LMA) MSW solutions [9], or the vacuum (VAC) neutrino oscillation solution [12]. We also assume the correctness of the four operating solar neutrino experiments, which fix the best-fit neutrino mixing parameters,  $\Delta m^2$  and  $\sin^2 2\theta$ . Using these best-fit parameters, we compute the expected event rates in future experiments. Assigning random errors of plausible size to future measurements we analyze together the four pioneering experiments that have been performed and the simulated new experiments. We establish 95% confidence limits on neutrino parameters that are consistent with the four operating experiments, and with simulated results of future experiments, using the techniques described previously in [11].

## II. NEUTRINO-ELECTRON SCATTERING EXPERIMENTS

In this section, we determine by how much measurements of the rates of neutrino-electron scattering by  ${}^7\text{Be}$  or *pep* neutrino lines can reduce the allowed regions in the neutrino mass versus neutrino mixing angle plane. The neutrino-electron scattering reaction can be represented by the equation

$$\nu + e \rightarrow \nu' + e'. \quad (3)$$

Neutrino-electron scattering experiments are sensitive to both charged current (i.e., only  $\nu_e$ ) and neutral current (i.e., all neutrino flavors) interactions. For the  ${}^7\text{Be}$  line, the ratio of the total electron neutrino scattering cross section to the total neutral current cross section is 4.53. For the *pep* line, the corresponding ratio of the cross sections is 4.93. All of the results

given in this paper include radiative corrections according to the perscription of reference [30].

Table II gives the recoil electron event rates in SNU predicted by different solutions of the solar neutrino problem for individual neutrino sources. The neutrino oscillation parameters used in Table II were found by requiring that  $\chi^2$  be a minimum for the four experimental results described in Table I. The neutrino parameters differ slightly from those found in reference [11] because in the present paper we include radiative corrections for neutrino-electron scattering. The standard model fluxes are from reference [24].

### A. Recoil Electron Spectrum

Figure 1 shows the calculated energy spectrum of the recoil electrons for five conceivable scenarios: the standard solar model and no neutrino oscillations (indicated by the solid line), the SMA MSW solution (the dotted line), the LMA MSW solution (the short dashed line), and the vacuum neutrino oscillation solution (long dashed line). We also show the result for the extreme case [31,32] in which the solar luminosity is assumed to be produced by CNO reactions (the dot-dash curve).

The vertical axis of Figure 1 gives the calculated event rate in SNU per MeV, where 1 SNU is  $10^{-36}$  interaction per target electron per sec. The horizontal axis,  $T_e$ , is the kinetic energy of the recoil electron. Radiative corrections [30] are included in the cross section calculations.

For neutrino-electron scattering, 1 SNU is approximately 2.6 events per 100 tons per day (for a target material in which the mass number,  $A$ , equals twice the atomic number,  $Z$ ).

If neutrino oscillations do not occur, then the computed shape of the recoil electron spectrum for standard solar model fluxes has prominent sharp shoulders at the maximum kinetic energies of the  $^7\text{Be}$  and the *pep* neutrino lines, respectively, i.e., at 1.225 MeV and 0.665 MeV. These features are apparent for the standard model spectrum (solid line) in Figure 1. The large continuum contribution from *pp* neutrinos is confined to energies less

than 0.261 MeV. The  $^{13}\text{N}$  and  $^{15}\text{O}$  continuum neutrinos can produce maximum electron recoil kinetic energies of 0.988 MeV and 1.509 MeV, respectively. The rare  $^8\text{B}$  neutrinos produce a low-level continuum up to 14 MeV.

As shown by many authors [33], the neutrino-electron scattering rate may be much lower than in the standard solar model predictions if neutrino oscillations occur.

For the CNO solution, the predicted event rates for energies less than 1.5 MeV are larger than if standard model neutrino fluxes are assumed [32]. In the energy region in which the  $^7\text{Be}$  line produces electron recoils, the calculated event rate is larger by typically a factor of about 2.5 than what is expected from the standard solar model. Even greater enhancements in the predicted event rates, a factor of 7 or more, are implied by the CNO scenario in the region 0.7 MeV to 1.2 MeV, in which the electron recoils from scattering by the *pep* neutrino line are found.

## B. Allowed Regions of Neutrino Parameter Space

We begin this subsection by stating an important result that refers to all three of the neutrino oscillation scenarios. By a series of detailed calculations, we have found that a measurement of the electron scattering rate of either the  $^7\text{Be}$  0.862 MeV line or the *pep* line to an accuracy of 10% would, in conjunction with the four operating experiments, essentially eliminate the two competing oscillation scenarios that are assumed, for purpose of that particular simulation, not to be correct. Thus, for example, if the SMA scenario is assumed to be correct and either the  $^7\text{Be}$  or the *pep* line is measured to a 10% accuracy, then both the LMA and the vacuum oscillation scenarios will be ruled out. Experiments with a much improved accuracy of 5% do not provide significantly more stringent constraints on allowable oscillations hypotheses.

Neutrino-electron scattering experiments can determine which, if any, neutrino oscillation scenario is correct.

Table III gives the predicted results for future experiments on solar neutrino lines that

are implied by the best-fit oscillation descriptions of the four pioneering solar neutrino experiments. The predicted event rates and confidence limits for neutrino-electron scattering were computed using the techniques of reference [11] and the standard model fluxes of reference [24].

The results of our more specific calculations for neutrino-electron scattering experiments are summarized in Figure 2a-c. The regions in the mass versus mixing angle plane that are allowed by the four operating solar neutrino experiments are delineated by the solid lines in Figure 2, which are taken from [11]. Assuming 10% experimental errors for future measurements, the dotted lines show the smaller allowed regions if a measurement of the  ${}^7\text{Be}$  line rate is made. If a *pep* measurement is also made, the allowed regions are reduced still further to the regions indicated by the dashed lines. In all cases, we determine the 95% C.L. by requiring that the boundaries of the allowed region satisfy  $\chi^2 = 5.99 + \chi^2_{\min}$ .

The top panel, Figure 2a, was constructed assuming the correctness of the best-fit small mixing angle solution of the solar neutrino problem. The dark circle shows the position in the mass and mixing angle plane of the best-fit solution and the dark line shows the 95% confidence limits of the parameters determined by a  $\chi^2$  fit to the results of the four pioneering solar neutrino experiments. With the four published experimental results, the large mixing angle solution is also allowed.

A measurement of the scattering rate of neutrinos from the 0.862 MeV  ${}^7\text{Be}$  line would, with the given assumptions, eliminate the large mixing angle solution and reduce significantly the allowed area of the small mixing angle solution. The additional measurement of the *pep* line would reduce only slightly the allowed region.

The middle panel of Figure 2b refers to the case in which the large mixing angle solution is correct. The allowed region for the SMA solution with just the four operating experiments is slightly larger in Figure 2b than in Figure 2a, because for the LMA solution adopted in the middle panel  $\chi^2_{\min, \text{LMA}} = 2.5$  whereas for the SMA solution the fit is much better,  $\chi^2_{\min, \text{SMA}} = 0.3$ .

A  ${}^7\text{Be}$  measurement would reduce significantly the allowed range of LMA parameters

and almost entirely eliminate the permitted SMA parameter space, as can be seen from Figure 2b. The vacuum oscillation solution would also be ruled out. Adding a measurement of the *pep* line would, in this case, significantly reduce the remaining parameter space. All that would be left would be a relatively small region surrounding the best-fit LMA solution.

Finally, we show in Figure 2c the potential results assuming the correctness of the vacuum neutrino oscillations. The best-fit value of  $\chi^2_{\min, \text{VAC}} = 2.5$ . In this case, the  ${}^7\text{Be}$  line measurement greatly reduces the allowed parameter space for the vacuum oscillations and completely eliminates the SMA and LMA MSW solutions. The *pep* measurement makes a further dramatic reduction of the allowed parameter space, centering the overall allowed region on a small area closely surrounding the best-fit point determined from the four existing experiments.

### C. Summary of Potential of Neutrino-Electron Scattering Experiments

We conclude this section with a brief summary of what can be learned from neutrino-electron scattering experiments using the  ${}^7\text{Be}$  and *pep* neutrino lines. The electron recoil spectra expected, see Figure 1, are different depending upon whether the sun shines by *pp* or CNO fusion reactions. If the CNO cycle is the dominant source of energy generation, the expected event rate is larger in the region in which the electron recoil energy is less than 1.5 MeV and the shape and energy span of the recoil electron energy spectrum is different, than would be expected if *pp* reactions are most important source of solar energy generation.

An accurate measurement of the scattering rate of the  ${}^7\text{Be}$  or the *pep* line would allow only one of the three popular neutrino oscillation scenarios. If the  ${}^7\text{Be}$  line is measured, then the additional measurement of the *pep* line would provide a major further reduction in the allowed range of neutrino parameters if either the LMA or the vacuum oscillation solution is correct. If the SMA solution has been chosen by Nature, then the *pep* line may not add much additional information.

### III. ABSORPTION PLUS ELECTRON SCATTERING EXPERIMENTS

In this section, we show how a neutrino absorption (charged-current) experiment, when combined with an electron scattering experiment, makes possible the measurement of the neutrino survival probability at a specific energy. Relevant neutrino-electron scattering experiments include BOREXINO [25], HERON [27], and HELLAZ [26], while Ga-As [28], and  ${}^7\text{Li}$  [34] are candidates for an absorption detector of the  ${}^7\text{Be}$  and *pep* neutrino lines. One advantage of a lithium detector in this connection is that the absorption cross sections are large and are accurately known [35] because the inverse reaction ( ${}^7\text{Be}$  electron capture) is well studied in the laboratory.

In III A, we present the formulae that determine the survival probability in terms of the measured rates of the absorption and scattering experiments. In the following subsection, III B, we present a graphical description of the allowed regions in the absorption-scattering plane that are permitted by the four operating solar neutrino experiments. Performing both an absorption and a scattering experiment using a neutrino line selects a unique point in the absorption-scattering plane (or, with experimental errors, a unique region) that determines the survival probability at the energy of the line.

In the formulae presented in this section and in Sections IV and V, we assume that there are no sterile neutrinos. In Section VII, we generalize the results to the case in which sterile neutrinos exist.

#### A. The Measurement of Survival Probabilities at a Specific Energy

Consider an electron-type neutrino with energy  $E_\nu$  that is created in the interior of the sun. We denote by  $P$  the probability that the neutrino remains an electron-type neutrino when it reaches a detector on earth, i.e.,  $P = P(\nu_e \rightarrow \nu_e; E_\nu)$ . In the literature,  $P$  is usually referred to as a “ $\nu_e$  survival probability.” The rate per target atom for the charged-current (absorption) reaction at energy  $E_\nu$  may be written

$$R_{\text{abs}} = \sigma_{\text{abs}} P \phi, \quad (4)$$

where  $\sigma_{\text{abs}}$  is the absorption cross section, and  $\phi$  is the total flux of neutrinos of energy  $E$  created in the sun. In what follows, we suppose that  $P$  is averaged over the neutrino production region in the interior of the sun. The rate per target electron for the electron scattering reaction is

$$R_{\text{esc}} = [\sigma_{\text{esc}}(\nu_e) - \sigma_{\text{esc}}(\nu_x)] P \phi + \sigma_{\text{esc}}(\nu_x) \phi, \quad (5)$$

where  $\sigma_{\text{esc}}$  is the electron scattering cross section and  $\nu_x$  is any normalized linear superposition of  $\nu_\mu$  and  $\nu_\tau$ .

Combining Eqs. 4 and 5, we obtain an explicit expression for the survival probability for electron-type neutrinos of energy  $E$ :

$$P = \frac{\sigma_{\text{esc}}(\nu_x) R_{\text{abs}}}{\sigma_{\text{abs}} R_{\text{esc}} - [\sigma_{\text{esc}}(\nu_e) - \sigma_{\text{esc}}(\nu_x)] R_{\text{abs}}} \quad (6)$$

Equation (6) could be used to determine, independent of any solar physics, the survival probability at a specific energy for neutrinos produced in either the  ${}^7\text{Be}$  or the *pep* line.

How well do experiments with specific uncertainties determine the survival probability? This question is answered by Eq. (7), which is shown below.

$$-\frac{\partial \ln P}{\partial \ln R_{\text{esc}}} = +\frac{\partial \ln P}{\partial \ln R_{\text{abs}}} = \frac{[(\sigma_{\text{esc}}(\nu_e) - \sigma_{\text{esc}}(\nu_x)) P + \sigma_{\text{esc}}(\nu_x)]}{\sigma_{\text{esc}}(\nu_x)}. \quad (7)$$

To estimate the accuracy with which  $P$  is determined by a given pair of experiments, one inserts the best-estimate of  $P$  obtained from Eq. (6) in the right hand side of Eq. (7). The fractional uncertainty in the inferred survival probability for given experimental errors can then be determined by multiplying Eq. (7) by the fractional uncertainty,  $\Delta R_{\text{esc}}/R_{\text{esc}}$ , in the measured neutrino-electron scattering rate or by the fractional uncertainty,  $\Delta R_{\text{abs}}/R_{\text{abs}}$ , in the measured neutrino absorption rate.

The uncertainty in the experimentally determined survival probability depends only upon the survival probability itself and upon the ratio of neutrino-electron scattering cross sections,  $\sigma_{\text{esc}}(\nu_e)/\sigma_{\text{esc}}(\nu_x)$ . For a very small inferred survival probability, the fractional uncertainty in the probability that results from a measurement with a specified fractional error is

equal to that fractional error. For survival probabilities close to unity, the fractional error in the inferred survival probability is amplified by a factor of  $\sigma_{\text{esc}}(\nu_e) / \sigma_{\text{esc}}(\nu_x)$  relative to the error in the measurement.

## B. Allowed Parameter Regions if Electron Scattering and Absorption are Measured

We can rewrite Eq. (6) as a linear relation between the neutrino-electron scattering rate and the charged current rate. Dividing Eq. (4) and Eq. (5) by the standard model expectations, one finds

$$\frac{R_{\text{esc}}}{R_{\text{esc,SSM}}} = \frac{R_{\text{abs}}}{R_{\text{abs,SSM}}} + \frac{\sigma_{\text{esc}}(\nu_x)(1 - P)}{\sigma_{\text{esc}}(\nu_e)}. \quad (8)$$

Figure 3 displays in the electron-scattering versus charged current plane the linear relation between the two measurable event rates. The upper panel of Fig. 3 shows the 95% C.L. regions that are allowed by the four operating experiments for the SMA and the LMA MSW solutions. The two sets of MSW solutions overlap slightly but are well separated from the predictions of the standard model. The lower panel of Fig. 3 shows the relatively larger range that is allowed by the vacuum oscillation solutions.

Figure 4 displays similar information for the *pep* line. Note that the upper panel of Fig. 4 shows that the SMA and the LMA solutions are distinguishable if both the charged current and the electron scattering rates are measured for the *pep* line. The allowed range of vacuum solutions is, however, very large, as is shown by the lower panel of Fig. 4.

Figure 3 and Figure 4 illustrate visually how one can, with the help of Eq. (8), and measurements of the neutrino absorption and electron scattering rates, determine the survival probability  $P$  at a given energy.

## IV. NEUTRAL CURRENT EXPERIMENTS

Raghavan, Pakvasa, and Brown [36] proposed studying the neutral current excitation of individual nuclear levels in the same detector in which the  $\nu_e$  flux was measured. As possible

targets, they suggested  $^{11}\text{B}$ ,  $^{40}\text{Ar}$ , and  $^{35}\text{Cl}$ , all of which are sensitive to the continuum neutrinos from  $^8\text{B}$  beta decay in the sun. In a more recent study, Raghavan, Raghavan, and Kovacs [37] proposed using a 4 ton LiF detector with potentially keV energy resolution to study neutral current and charged current solar neutrino reactions. Most recently, Bowles and Gavrin [28] have proposed using neutral current excitations of  $^{71}\text{Ga}$ ,  $^{69}\text{Ga}$ , and  $^{75}\text{As}$  to help diagnose the composition of the solar neutrino spectrum.

Let us consider as an especially promising example the neutral current excitation of the first excited state of  $^7\text{Li}$ , which lies 0.478 MeV above the ground state of  $^7\text{Li}$ . The neutral current excitation can be represented by the equation

$$\nu + {}^7\text{Li} \rightarrow \nu' + {}^7\text{Li}^*. \quad (9)$$

The reaction can be observed by detecting the 0.478 MeV de-excitation  $\gamma$ -rays. The energy threshold for this reaction is sufficiently low that both the higher-energy (0.862 MeV)  ${}^7\text{Be}$  line and the *pep* neutrinos can excite reaction (9). The *pp* neutrinos and the lower-energy (0.384 MeV)  ${}^7\text{Be}$  neutrinos are not sufficiently energetic to cause reaction (9). The  ${}^8\text{B}$ ,  ${}^{13}\text{N}$ , and  ${}^{15}\text{O}$  neutrinos, as well as  ${}^7\text{Be}$  and *pep* neutrinos, can all contribute to the total observed neutrino excitation of  ${}^7\text{Li}$ .

The neutral current matrix element for reaction (9) is large and is known accurately [37] since the matrix element for reaction (9) is, by isotopic spin invariance, the same as the matrix element for the observed superallowed decay from the ground state of  ${}^7\text{Be}$  to the first excited state of  ${}^7\text{Li}$ .

If both the neutral current excitation and the charged current absorption could be measured for the same neutrino line, then the survival probability for neutrinos with the energy of the line would be given by the simple formula

$$P = \frac{\sigma_{\text{NC}} R_{\text{abs}}}{\sigma_{\text{abs}} R_{\text{NC}}}. \quad (10)$$

Here  $R_{\text{abs}}$  and  $R_{\text{NC}}$  are the reaction rates per target particle of the charged current (absorption) and neutral current processes. The sensitivity with which the survival probability could be determined would be given by the following relation,

$$\frac{\partial \ln P}{\partial \ln R_{\text{abs}}} = -\frac{\partial \ln P}{\partial \ln R_{\text{NC}}} = 1.0. \quad (11)$$

If the neutral current measurement were combined with an electron-scattering measurement, then the survival probability would be

$$P = \frac{\sigma_{\text{NC}} R_{\text{esc}} - \sigma_{\text{esc}}(\nu_x) R_{\text{NC}}}{[\sigma_{\text{esc}}(\nu_e) - \sigma_{\text{esc}}(\nu_x)] R_{\text{NC}}}. \quad (12)$$

The sensitivity with which the survival probability would be determined is

$$\frac{\partial \ln P}{\partial \ln R_{\text{esc}}} = -\frac{\partial \ln P}{\partial \ln R_{\text{NC}}} = \frac{\sigma_{\text{esc}}(\nu_e) P + \sigma_{\text{esc}}(\nu_x)(1-P)}{[\sigma_{\text{esc}}(\nu_e) - \sigma_{\text{esc}}(\nu_x)] P}. \quad (13)$$

In the limit in which  $P$  is very small, Eq. (13) shows that the survival probability cannot be determined by a combination of a neutral current measurement and an electron scattering measurement. The physical reason for this indeterminacy, indicated by the presence of  $P$  in the denominator of Eq. (13), is that both the neutral current rate and the electron scattering rate depend only on the neutral current interaction when the survival probability is very small.

If all three processes, electron-neutrino scattering, neutrino absorption, and neutral-current excitation were measured for the same neutrino line, then the survival probability would be over-determined by Eq. (6), Eq. (10), and Eq. (12). The extra constraints could be used as a test of the self-consistency of the experimental measurements.

Unfortunately, neutral current excitations like that shown in reaction (9) do not register the energy of the neutrino that causes the interaction. In this respect, neutral current excitations are similar to radiochemical solar neutrino experiments; they measure the sum of the reaction rates due to all the neutrino sources above the energy threshold. It seems likely [37], with our current expectations for the low energy fluxes of solar neutrinos (based upon the standard solar model and existing neutrino oscillation solutions), that the neutral current excitation of  ${}^7\text{Li}$  is dominated by the higher-energy  ${}^7\text{Be}$  branch. However, to verify or improve these expectations, additional observational information must be obtained from neutrino absorption experiments or from neutrino-electron scattering experiments that can identify the fluxes from individual neutrino sources.

As emphasized by previous authors [36,37], the principal role at present of a neutral current excitation experiment is to provide a measure of the total neutrino reaction rate, independent of neutrino flavor, for the entire solar neutrino spectrum. Since neutral current excitation experiments cannot be used at present to isolate the contribution of an individual line, we will not discuss these excitation experiments further in this paper.

## V. MODEL INDEPENDENT TESTS OF ELECTRON FLAVOR CONSERVATION

What can be learned about electron flavor conservation and neutrino parameters by combining the results, for a neutrino line, of an absorption experiment and a neutrino-electron scattering experiment? In answering this question, we present numerical results for  $N$ , the normalized ratio of neutrino electron scattering rate to neutrino absorption rate<sup>3</sup>,

$$N \equiv \frac{[\sigma_{\text{abs}}(\nu_e) R_{\text{esc}}]}{[\sigma_{\text{esc}}(\nu_e) R_{\text{abs}}]}. \quad (14)$$

Both  $R_{\text{esc}}$  and  $R_{\text{abs}}$  are proportional to the total neutrino flux created in the sun and therefore the absolute value of the flux cancels out of the ratio  $N$ . If electron neutrino flavor is conserved, then  $N \equiv 1.0$  independent of any solar physics. The quantity  $N$  plays much the same role for neutrino-electron scattering and neutrino absorption as does the ratio of neutral current to charged current rates that is a primary goal, for the higher energy <sup>8</sup>B neutrinos, of the SNO solar neutrino experiment.

If experimental measurements show that  $N$  is different from unity, then that would be a

---

<sup>3</sup> Equation (14) has exactly the same form as the expression, Eq. (10), for the survival probability as determined from a neutral current and an absorption measurement. Everything that we calculate in this section for  $N$  could be calculated for the survival probability defined by Eq. (10). We chose to carry out our numerical calculations for neutrino-electron scattering rather than neutral current excitation because neutrino-electron scattering experiments are currently being developed, whereas there is not yet an advanced proposal to detect neutral current excitations.

direct proof that electron flavor is not conserved. We consider in this section what can be learned from experiments with the 0.862 MeV  ${}^7\text{Be}$  and  $pep$  lines.

Table IV presents the values for  $N({}^7\text{Be})$  and  $N(pep)$  that are predicted by the best-fit oscillation solutions to the four operating solar neutrino experiments. The uncertainties indicated represent the 95% C.L. as defined in [11]. Most of the expected solution space is well separated from the prediction of electron flavor conservation, although there are relatively small regions of parameter space, especially for the LMA and vacuum oscillation solutions, in which the measured value of  $N$  would be indistinguishable from the value of 1.0 predicted by electron flavor conservation.

Figure 5 shows the allowed region in the  $N({}^7\text{Be})$  and  $N(pep)$  plane that is consistent with the four operating solar neutrino experiments at 95% C.L. Most of the area that is predicted to be occupied in the  $N({}^7\text{Be})$  and  $N(pep)$  plane is clearly separated from the point in the lower left hand corner at (1.0, 1.0) that is the standard model prediction. The upper panel of Figure 5 shows the solution space for the SMA and the LMA MSW solutions and the lower panel shows the solution space for the vacuum neutrino oscillations.

A priori one might expect to be able to determine the two neutrino oscillation parameters,  $\sin^2 2\theta$  and  $\Delta m^2$ , by measuring the two double ratios  $N({}^7\text{Be})$  and  $N(pep)$ . Unique solutions are obtainable for the SMA and vacuum oscillation solutions. In these two scenarios, the  ${}^7\text{Be}$  and  $pep$  lines are suppressed differently and the relative suppression of the two lines depends strongly on the neutrino oscillation parameters. However, for the LMA solution, the two lines are almost always nearly equally suppressed and there are many pairs of  $\sin^2 2\theta$  and  $\Delta m^2$  for which the suppression of the two lines is practically the same. If the LMA MSW solution is assumed to be correct, one cannot in general solve uniquely for the neutrino parameters using just the values of  $N({}^7\text{Be})$  and  $N(pep)$ .

How accurately can one determine neutrino parameters by measuring the two scattering to absorption ratios? This question is answered by Table V for MSW SMA oscillations and Table VI for vacuum oscillations.. The entries in the tables give the range of solutions for  $\Delta m^2$  and  $\sin^2 2\theta$  that are consistent at 95% C.L. with the four operating solar neutrino

experiments. If  $N(^7\text{Be})$  and  $N(\text{pep})$  are each measured to an accuracy of  $\pm 20\%$ , then one can read from Table V or Table VI the resulting accuracy with which  $\Delta m^2$  and  $\sin^2 2\theta$  and  $\Delta m^2$  will be known. For MSW oscillations (see Table V), the characteristic uncertainty in  $\Delta m^2$  would be about 10% and the characteristic uncertainty in  $\sin^2 2\theta$  would be a factor of three or less. For vacuum oscillations (see Table VI), the mixing angle would be determined well, typically to an accuracy of order 10% (although less well in some regions of parameter space). The mass difference is not as accurately determined for vacuum oscillations; the uncertainty indicated by Table VI can be as large as a factor of two, although there are some regions of parameter space in which the mass difference would be very well determined.

## VI. DO STERILE NEUTRINOS EXIST?

We discuss in Section VI A the modifications in the results previously presented that are required if sterile neutrinos exist. On a more theoretical level, we indicate in Section VI B how, in principle, the two solar neutrino lines that arise from  $^7\text{Be}$  electron capture can be used to test for the existence of sterile neutrinos<sup>4</sup>. Stimulating previous discussions of sterile neutrinos in the context of solar neutrino experiments can be found in references [28,29,38].

### A. Absorption Plus Electron Scattering Experiments

If sterile neutrinos exist, the flux of electron-type neutrinos is still given by  $P\phi$ , where the survival probability  $P = P(\nu_e \rightarrow \nu_e; E_\nu)$  and  $\phi$  is the total flux of neutrinos that are created in the sun. Thus the rate for the charged current absorption of neutrinos given by Eq. (4) has the same form whether or not sterile neutrinos exist. However, the total flux of

---

<sup>4</sup>We consider a general case in which sterile neutrinos can couple to  $\nu_e$ ,  $\nu_\mu$ , or  $\nu_\tau$ , and we consider probabilities  $P$  that refer to the net conversion (or survival) of electron type neutrinos which are created in the sun and detected on earth.

active neutrinos of all types will be reduced by a factor  $1 - P_{\text{sterile}} = 1 - P(\nu_e \rightarrow \nu_{\text{sterile}}; E_\nu)$ . If sterile neutrinos exist, the neutrino-electron scattering rate is

$$R_{\text{esc}} = [\sigma_{\text{esc}}(\nu_e) - \sigma_{\text{esc}}(\nu_x)] P\phi + \sigma_{\text{esc}}(\nu_x) (1 - P_{\text{sterile}}) \phi, \quad (15)$$

which reduces to Eq. (5) when  $P_{\text{sterile}} = 0$ . Combining Eq. (15) with Eq. (4), the survival probability in the presence of sterile neutrinos is

$$P = \frac{\sigma_{\text{esc}}(\nu_x) (1 - P_{\text{sterile}}) R_{\text{abs}}}{\sigma_{\text{abs}} R_{\text{esc}} - [\sigma_{\text{esc}}(\nu_e) - \sigma_{\text{esc}}(\nu_x)] R_{\text{abs}}}. \quad (16)$$

Comparing Eq. (16) with Eq. (6), we see that the true survival probability is smaller by a factor of  $(1 - P_{\text{sterile}})$  than the survival probability inferred by ignoring sterile neutrinos, i.e.,

$$P = (1 - P_{\text{sterile}}) P_{\text{no sterile } \nu\text{'s}}. \quad (17)$$

This reduction also applies if the survival probability  $P$  is determined by comparing the rates of neutral current excitation and charged current absorption, as summarized in Eq. (10). The relation given by Eq. (17) is physically obvious; it results from the fact that the survival probability is defined as the fraction of the total neutrino flux that remains electron-type neutrinos and that only  $(1 - P_{\text{sterile}})$  of the total flux is counted by measuring the interaction rates in neutral current experiments or in neutrino-electron scattering experiments.

The fractional uncertainties in the inferred survival probability can be calculated from equations that generalize Eq. (7), i.e.,

$$-\frac{\partial \ln P}{\partial \ln R_{\text{esc}}} = +\frac{\partial \ln P}{\partial \ln R_{\text{abs}}} = \frac{[(\sigma_{\text{esc}}(\nu_e) - \sigma_{\text{esc}}(\nu_x)) P + \sigma_{\text{esc}}(\nu_x) (1 - P_{\text{sterile}})]}{\sigma_{\text{esc}}(\nu_x) (1 - P_{\text{sterile}})}. \quad (18)$$

## B. A Test for the Existence of Sterile Neutrinos

The relative intensity of the two neutrino lines produced by electron capture on  ${}^7\text{Be}$  is determined by nuclear physics that is independent of the solar environment. The ratio

of the line strengths, the so-called branching ratio, has been determined accurately from laboratory experiments and is [39]

$$\frac{\phi(E_2)}{\phi(E_1)} = \text{Branching Ratio} = 0.115 , \quad (19)$$

where  $E_1 = 0.384$  MeV (10.3% of the total flux) and  $E_2 = 0.862$  MeV (89.7% of the total flux). We refer here to the familiar laboratory energies of the neutrino lines; the energies of the solar lines are increased by 1.24 keV and 1.29 keV, respectively [1].

For each of the lines, the total active neutrino flux can be obtained by measuring the neutrino-electron scattering rate and the charged-current absorption. One obtains from Eq. (4) and Eq. (16)

$$(1 - P_{\text{sterile}}) \phi = \frac{\sigma_{\text{abs}} R_{\text{esc}} - [\sigma_{\text{esc}}(\nu_e) - \sigma_{\text{esc}}(\nu_x)] R_{\text{abs}}}{\sigma_{\text{abs}} \sigma_{\text{esc}}(\nu_x)} . \quad (20)$$

Combining Eq. (19) and Eq. (20), we obtain for the measured ratio of the total neutrino flux at two different neutrino energies,

$$\frac{1 - P_{\text{sterile}}(E_1)}{1 - P_{\text{sterile}}(E_2)} = 0.115 \frac{X(E_1)}{X(E_2)} , \quad (21)$$

where

$$X \equiv \frac{\sigma_{\text{abs}} R_{\text{esc}} - [\sigma_{\text{esc}}(\nu_e) - \sigma_{\text{esc}}(\nu_x)] R_{\text{abs}}}{\sigma_{\text{abs}} \sigma_{\text{esc}}(\nu_x)} . \quad (22)$$

Let

$$\zeta \equiv \frac{[\sigma_{\text{esc}}(\nu_e) - \sigma_{\text{esc}}(\nu_x)] R_{\text{abs}}}{\sigma_{\text{abs}} R_{\text{esc}}} , \quad (23)$$

then the fractional uncertainties in the values of  $X$  from given experimental uncertainties can be calculated from

$$\frac{\partial \ln X}{\partial \ln R_{\text{abs}}} = -\zeta \frac{\partial \ln X}{\partial \ln R_{\text{esc}}} = \frac{-\zeta}{1 - \zeta} . \quad (24)$$

If sterile neutrinos exist, and the probability of their being created depends upon energy, then the ratio of measured quantities given in Eq. (21) must be different from unity. If  $P_{\text{sterile}}$

is a constant independent of energy, then the ratio in Eq. (21) will also equal unity. This latter result describes the fact that a theory with a constant  $P_{\text{sterile}}$  cannot be distinguished experimentally from a theory in which all of the solar neutrino fluxes are reduced by a constant factor. In this very special case of an energy-independent  $P_{\text{sterile}}$ , one would have to rely on solar model calculations of the total neutrino flux in order to determine if sterile neutrinos exist.

In very interesting discussions, Calabresu, Fiorentini, and Lissia [38] and Bowles and Gavrin [28] have pointed out that one can also test for the existence of sterile neutrinos if one accepts the (robustly calculated) standard solar model ratio of the total flux of *pep* neutrinos to the total flux of *pp* neutrinos. In this case, one obtains a relation similar to Eq. (21) for *pep* and *pp* by replacing in Eq. (21) the  ${}^7\text{Be}$  branching ratio of 0.115 with the standard solar model branching ratio of  $2.4 \times 10^{-2}$  for *pep* to *pp* neutrinos.

## VII. SUMMARY AND DISCUSSION

The first three decades of solar neutrino research concentrated on continuum energy spectra. Our goal is to focus additional attention on what can be learned from studying solar neutrino lines. We illustrate what may be observed by assuming the correctness of the different neutrino oscillation solutions that fit the four operating solar neutrino experiments. For all of our considerations, we assume the existence of experiments with the excellent energy resolution that is necessary to separate solar neutrino lines from continuum solar neutrino sources and from background events.

We explore first what neutrino-electron scattering experiments can tell us about the MSW and vacuum neutrino oscillation solutions to the solar neutrino problems. We find (see Figure 2) that a measurement of the scattering rate of either the (0.862 MeV)  ${}^7\text{Be}$  line or the *pep* neutrino line would, when combined with the results from the operating experiments, eliminate all but one of the popular neutrino oscillation scenarios. Which particular solution is permitted in our simulation is, of course, determined by which of the

three solutions (small angle MSW, large angle MSW, or vacuum oscillations) that we assume is correct. As is shown in Figure 2, a measurement of the *pep* line in addition to the  ${}^7\text{Be}$  line would in many cases provide a significant reduction of the domain of allowed neutrino parameters over what is possible by studying only the  ${}^7\text{Be}$  line.

The “all CNO” scenario for solar nuclear energy generation predicts (see Figure 1) measurably higher event rates below 1.5 MeV and a markedly different shape for the electron recoil energy spectrum than would be expected, with or without neutrino oscillations, for the standard “*pp*-dominated” solar model description of the energy generation. Even without obtaining a high-statistics measurement of the possibly depleted (by oscillations)  ${}^7\text{Be}$  neutrino flux, a measurement of the electron recoil energy spectrum below 1.5 MeV could test the “all CNO” scenario experimentally.

The quantitative predictions of what is expected for neutrino-electron scattering experiments are summarized in Table II, Table III and Figure 2. These predictions can be tested by the BOREXINO [25], HELLAZ [26], and HERON [27] experiments.

What can be learned about neutrino properties if both the charged-current reaction rate (neutrino absorption) and the neutrino-electron scattering rate are measured? The short answer is: one can determine the survival probability for electron-type neutrinos at the energy of the neutrino line. Equation (6) expresses the survival probability in terms of the measured event rates for the absorption and the scattering experiments and Eq. (7) shows how accurately the survival probability can be determined for specified experimental errors. If both the scattering and absorption rates are measured, the results lie along a line in the absorption-scattering plane. The predicted range of the solutions for the small and large angle MSW solutions are well separated from the standard model predictions, as is shown in Figure 3a for (0.862)  ${}^7\text{Be}$  neutrinos and in Figure 4a for *pep* neutrinos. Most, but not all, of the vacuum oscillation solutions that are consistent with the four operating experiments are well separated from the standard model solution, as shown in Figure 3b and Figure 4b. For the *pep* neutrinos, the small angle and large angle MSW solutions are separated from each other in the absorption-scattering plane. For the  ${}^7\text{Be}$  neutrinos, there is some overlap

in the predicted domain for the small and large angle solutions.

If neutrino oscillations occur, there is a factor of about 5 uncertainty in the expected neutrino-electron scattering rates for both the  ${}^7\text{Be}$  and the *pep* lines. Table III shows that neutrino oscillation solutions that are consistent with the four operating experiments permit, at 95% C.L., the rate for the 862 keV  ${}^7\text{Be}$  line to be anywhere between 22% and 98% of the standard model prediction and the 1.442 MeV *pep* rate to lie between 21% and 98% of the standard model prediction. The 384 MeV  ${}^7\text{Be}$  line, which may be between 34% and 100% of the standard prediction, is difficult to observe because of the intense background from the *p-p* solar neutrinos.

Neutral current excitations of individual nuclear levels can, as first proposed by Raghavan, Pakvasa, and Brown [36], provide important information about the total neutrino flux, independent of neutrino flavor. Like radiochemical experiments, neutral current excitations provide only one measured number, the total rate due to all neutrino sources. In order to interpret neutral current excitations, one has to make use of theoretical calculations involving the standard solar model and the oscillation scenarios. We describe in Section IV what can be learned from neutral current excitation experiments at present and what might be possible in the future. We signal out as especially promising for a future experiment the neutrino excitation of the 0.478 MeV first excited state of  ${}^7\text{Li}$ . The superallowed matrix element for this transition is large and is known accurately. Raghavan, Raghavan, and Kovacs [37] have suggested that a practical solar neutrino experiment could be carried out with a 4 ton LiF detector. The fluorine in a LiF detector could make possible a simultaneous study at high energy resolution of the higher-energy  ${}^8\text{B}$  solar neutrinos [40].

Model-independent tests of neutrino flavor conservation can be carried out by combining the results of an absorption experiment and a neutrino-electron scattering experiment for a given neutrino line. The ratio [see Eq. (14)] of the measured neutrino-electron scattering rate to the measured neutrino absorption rate, normalized by the interaction cross sections, must be equal to unity if electron neutrino flavor is conserved. Any measured value that is significantly different from 1.0 would be a direct proof that electron neutrino flavor is not

conserved.

Table IV presents, for different neutrino oscillation scenarios, the best-estimates and the 95% C.L. predictions for the normalized ratio of neutrino electron scattering to neutrino absorption. For the small mixing angle MSW solution, the best-estimates are 15.1 and 11.7 for the  ${}^7\text{Be}$  and the *pep* lines, respectively, an order of magnitude different from what is predicted by neutrino flavor conservation.

Figure 5 shows for both the  ${}^7\text{Be}$  and the *pep* lines the wide range of values for the normalized ratio (scattering to absorption) that are consistent at 95% C.L. with the results of the four operating solar neutrino experiments. Only a small fraction of the allowed solution space is close to the region (both normalized ratios equal to unity) that is implied by electron flavor conservation. Thus a measurement of neutrino absorption and neutrino electron scattering for one (or both) of the strong neutrino lines would provide a model-independent demonstration of electron flavor non-conservation, if the neutrino oscillation fits to the results of the four operating experiments contain the solution to the solar neutrino problems.

We show in Section VIA how the results of the previous sections must be modified if there exist sterile neutrinos that are coupled to electron type neutrinos. The general result is that the true electron neutrino survival probability in the presence of sterile neutrinos is smaller by a factor of  $1 - P_{\text{sterile}}$  than the survival probability inferred by neglecting the possible existence of sterile neutrinos.

Do sterile neutrinos exist? One can in principle carry out a model-independent test for the existence of sterile neutrinos by combining two experiments for each of the two  ${}^7\text{Be}$  neutrino lines. One knows the branching ratio for the two lines from laboratory measurements and this ratio only depends upon nuclear physics. Equation (21) shows that one can detect an energy-dependent probability for transition to a sterile neutrino by measuring the absorption and the scattering rate for both of the  ${}^7\text{Be}$  neutrino lines. However, it will be difficult to study the lower energy  ${}^7\text{Be}$  line because of the background from *pp* neutrinos. If one accepts as correct the robustly-calculated standard solar model ratio of *pep* to *pp*

neutrino fluxes, then one can apply [38,28] the same argument as described here for  ${}^7\text{Be}$  neutrinos [and therefore Eq. (21)] to test for the existence of sterile neutrinos.

#### ACKNOWLEDGMENTS

J.N.B. acknowledges support from NSF grant #PHY95-13835. The work of P.I.K. was partially supported by funds from the Institute for Advanced Study. This investigation was initially sparked by a question asked by F. Calaprice and by R. Raghavan; the question was: how much more could BOREXINO learn about neutrino physics if the *pep* neutrinos were measured in addition to the  ${}^7\text{Be}$  neutrinos? We are grateful to R. Eisenstein and E. Lisi for valuable comments and discussions.

## REFERENCES

- [1] J. N. Bahcall, Phys. Rev. D **49**, 3923 (1994); J. N. Bahcall, Phys. Rev. Lett. **71**, 2369 (1993).
- [2] B. T. Cleveland *et al.*, Nucl. Phys. B (Proc. Suppl.) **38**, 47 (1995); R. Davis, Prog. Part. Nucl. Phys. **32**, 13 (1994).
- [3] KAMIOKANDE Collaboration, Y. Suzuki, Nucl. Phys. B (Proc. Suppl.) **38**, 54 (1995); K. S. Hirata *et al.*, Phys. Rev. D **44**, 2241 (1991).
- [4] GALLEX Collaboration, P. Anselmann *et al.*, Phys. Lett. B **327**, 377 (1994); **342**, 440 (1995); **357**, 237 (1995).
- [5] SAGE Collaboration, G. Nico *et al.*, in *Proceedings of the XXVII International Conference on High Energy Physics*, Glasgow, Scotland, 1994, edited by P. J. Bussey and I. G. Knowles (Institute of Physics, Bristol, 1995), p. 965; J. N. Abdurashitov *et al.*, Phys. Lett. B **328**, 234 (1994).
- [6] M. Takita, in *Frontiers of Neutrino Astrophysics*, edited by Y. Suzuki and K. Nakamura (Universal Academy Press, Tokyo, 1993), p. 147; T. Kajita, *Physics with the SuperKamiokande Detector*, ICRR Report 185-89-2 (1989).
- [7] H. H. Chen, Phys. Rev. Lett. **55**, 1534 (1985); G. Ewan *et al.*, Sudbury Neutrino Observatory Proposal, SNO-87-12 (1987); A. B. McDonald, in Proceedings of the Ninth Lake Louise Winter Institute, edited by A. Astbury *et al.* (World Scientific, Singapore, 1994), p. 1.
- [8] S. L. Glashow, Nucl. Phys. **22**, 579 (1961); S. Weinberg, Phys. Rev. Lett. **19**, 1264 (1967); A. Salam, in *Elementary Particle Theory*, edited by N. Svartholm (Almqvist and Wiskells, Stockholm, 1968) p. 367.
- [9] L. Wolfenstein, Phys. Rev. D **17**, 2369 (1978); S. P. Mikheyev and A. Yu. Smirnov, Yad. Fiz. **42**, 1441 (1985), [Sov. J. Nucl. Phys. **42**, 913 (1985)].

[10] N. Hata and P. Langacker, Phys. Rev. D **50**, 632 (1993); G. Fogli, E. Lisi, and D. Montanino, Phys. Rev. D. **49**, 3226 (1994); E. Gates, L. Krauss, and M. White, Phys. Rev. D. **51**, 2631 (1995); P. Krastev and S. T. Petcov, Nucl. Phys. B **449**, 605 (1995).

[11] J. N. Bahcall and P. I. Krastev, Phys. Rev. D **53**, 4211 (1996).

[12] V. N. Gribov and B. M. Pontecorvo, Phys. Lett. B **28**, 493 (1969); J. N. Bahcall and S. C. Frautschi, Phys. Lett. B **29**, 623 (1969).

[13] J. N. Bahcall, N. Cabibbo, and A. Yahil, Phys. Rev. Lett. **28**, 316 (1972).

[14] Z. G. Berezhiani and M. I. Vysotsky, Phys. Lett. B **199**, 281 (1987).

[15] M. B. Voloshin, M. I. Vysotskii, and L. B. Okun, Soviet Phys. JETP **64**, 446 (1986); *erratum*, **65**, 209 (1987).

[16] C.-S. Lim and W. J. Marciano, Phys. Rev. D **37**, 1368 (1988).

[17] E. K. Akhmedov, Phys. Lett. B **213**, 64 (1988).

[18] M. Gasperini, Phys. Rev. D **38**, 2635 (1988).

[19] E. Roulet, Phys. Rev. D **44**, R935 (1991).

[20] M. M. Guzzo, A. Masiero, and S. T. Petcov, Phys. Lett. B **260**, 154 (1991).

[21] J. N. Bahcall, R. Davis, Jr., P. Parker, A. Smirnov, and R. Ulrich, editors: “Solar Neutrinos, The First Thirty Years,” Frontiers in Physics, Vol. 92 (Addison-Wesley, 1994).

[22] J. N. Bahcall, Phys. Rev. D **41**, 2964 (1990).

[23] J. N. Bahcall, Neutrino Astrophysics (Cambridge University Press, Cambridge, England, 1989).

[24] J. Bahcall and M. Pinsonneault, Rev. Mod. Phys. **67**, 1 (1995).

[25] C. Arpesella *et al.*, BOREXINO proposal, Vols. 1 and 2, edited by G. Bellini, *et al.* (Univ. of Milano, Milano, 1992); R. S. Raghavan, Science **267**, 45 (1995).

[26] G. Laurenti *et al.*, in *Proceedings of the Fifth International Workshop on Neutrino Telescopes, Venice, Italy, 1993*, edited by M. Baldo Ceolin (Padua University, Padua, Italy, 1994), p. 161; G. Bonvicini, Nucl. Phys. B **35**, 438 (1994).

[27] S. R. Bandler *et al.*, Journal of Low Temp. Phys. **93**, 785 (1993); R. E. Lanou, H. J. Maris, and G. M. Seidel, Phys. Rev. Lett. **58**, 2498 (1987).

[28] T. J. Bowles and V. N. Gavrin, talk presented at the *Seventh International Workshop on Neutrino Telescopes, Venice, Italy, February 28, 1996*.

[29] S. M. Bilenky and C. Giunti, Phys. Lett. B **311**, 179 (1993); **320**, 323 (1994); Astropart. Physics **2**, 353 (1994).

[30] J. N. Bahcall, M. Kamionkowski, and A. Sirlin, Phys. Rev. D. **51**, 6146 (1995).

[31] H. A. Bethe, Phys. Rev. **55**, 434 (1939).

[32] J. N. Bahcall, M. Fukugita, and P. I. Krastev, Phys. Lett. B. **374**, 1 (1996).

[33] J. M. Gelb, W. Kwong, and S. P. Rosen, Phys. Rev. Lett. **69**, 1864 (1992); P. I. Krastev and S. T. Petcov, Phys. Lett. B **338**, 99 (1993); N. Hata and P. Langacker, Phys. Rev. D **50**, 632 (1994); W. Kwong and S. P. Rosen, Phys. Rev. Lett. **73**, 369 (1994); J. N. Bahcall, Phys. Lett. B **338**, 276 (1994); E. Gates, L. M. Krauss, and M. White, Phys. Rev. D **51**, 2631 (1995); E. Calabresu, N. Ferrari, G. Fiorentini, and M. Lissia, Astropart. Phys. **4**, 159 (1995); J. N. Bahcall and P. I. Krastev, Phys. Rev. D **53**, 4211 (1996).

[34] F. Fontanelli, M. Galeazzi, F. Gatti, P. Meunier, A. Swift, and S. Vitale, Nucl. Instruments and Methods in Physics Research A **370**, 273 (1996); S. N. Danshin, A. V. Kopylov, A. N. Likhovid, E. A. Yanovich, and G. T. Zatsepin, in *Proceedings of the*

*Fifth International Workshop on Neutrino Telescopes, Venice, Italy, 1993*, edited by M. Baldo Ceolin (Padua University, Padua, Italy), p. 137 (1994); J. N. Bahcall, Phys. Rev. Lett. **23**, 251 (1969).

- [35] J. N. Bahcall, Rev. Mod. Phys. **50**, 881 (1978).
- [36] R. S. Raghavan, S. Pakvasa, and B. A. Brown, Phys. Rev. Lett. **57**, 1801 (1986).
- [37] R. S. Raghavan, P. Raghavan, and T. Kovacs, Phys. Rev. Lett. **71**, 4295 (1986).
- [38] E. Calabresu, G. Fiorentini, and M. Lissia, Astroparticle Physics (1996), submitted.
- [39] *Table of Isotopes*, edited by C. M. Lederer and V. S. Shirley (Wiley, New York, 1978), p.3; F. Ajzenberg-Selove, Nucl. Phys. A **490**, 1 (1988).
- [40] See discussion on pgs. 416-418 of [23].
- [41] J. N. Bahcall, Phys. Rev. Lett. **23**, 251 (1969).

## TABLES

TABLE I. Experimental results for four operating experiments. The experimental results are given in SNU for all of the experiments except Kamiokande, for which the result is expressed as the measured  ${}^8\text{B}$  flux in units of  $\text{cm}^{-2}\text{s}^{-1}$  at the earth, assuming the standard model neutrino shape. The ratios of the measured values to the corresponding predictions in the standard solar model of ref. [24] are also given. The result cited for the Kamiokande experiment assumes that the shape of the  ${}^8\text{B}$  neutrino spectrum is not affected by physics beyond the standard electroweak model. Here 1 SNU is defined as  $10^{-36}$  interactions per target atom per sec [41].

Experiment	Result ( $\pm 1\sigma$ )	Reference
HOMESTAKE	$2.55 \pm 0.17(\text{stat}) \pm 0.18(\text{syst})$ SNU	[2]
GALLEX	$77.1 \pm 8.5(\text{stat}) \pm^{+4.4}_{-5.4}(\text{syst})$ SNU	[4]
SAGE	$69 \pm 11(\text{stat})^{+5}_{-7}(\text{syst})$ SNU	[5]
KAMIOKANDE	$[2.89 \pm^{0.22}_{0.21}(\text{stat}) \pm 0.35(\text{syst})] \times 10^6 \text{ cm}^{-2}\text{s}^{-1}$	[3]

TABLE II. Recoil electron event rates in SNU from individual neutrino sources predicted by different solutions of the solar neutrino problem. The neutrino oscillation parameters in each solution have been assumed to be those providing a minimum  $\chi^2$  [11]. The standard model fluxes are from reference [24]. The threshold energy for recoil electron was set to zero in the calculations.

Solution	$pp$	$pep$	${}^7\text{Be}(0.862)$	${}^7\text{Be}(0.384)$	${}^8\text{B}$	${}^{13}\text{N}$	${}^{15}\text{O}$
SSM	6.7E+1	1.5E+0	2.7E+1	1.0E+0	3.9E-1	2.8E+0	3.8E+0
SMA	6.5E+1	3.3E-1	6.2E+0	8.2E-1	1.5E-1	9.0E-1	8.6E-1
LMA	4.8E+1	8.8E-1	1.7E+1	7.0E-1	1.5E-1	1.8E+0	2.2E+0
VAC	4.4E+1	3.6E-1	1.9E+1	3.8E-1	1.5E-1	1.7E+0	2.2E+0
CNO	2.2E-3	1.2E-4	1.7E-2	9.8E-1	1.4E-1	6.8E+1	6.2E+1

TABLE III. Best-fit neutrino oscillation predictions for neutrino-electron scattering. The best-fit (and 95% C.L. limits) are given for the ratio of the rate with neutrino oscillations to the rate with the unmodified standard solar model flux. The predicted event rates and confidence limits for neutrino-electron scattering are computed using the techniques of reference [11] and the standard model fluxes of reference [24].

Scenario	$\chi^2_{\text{min}}$	${}^7\text{Be}/({}^7\text{Be})_{\text{SSM}}$	${}^7\text{Be}/({}^7\text{Be})_{\text{SSM}}$	${}^{pep}/({}^{pep})_{\text{SSM}}$
		(0.862 MeV)	(0.384 MeV)	(1.442 MeV)
SMA	0.3	$0.23^{+0.30}_{-0.01}$	$0.81^{+0.19}_{-0.43}$	$0.22^{+0.11}_{-0.01}$
LMA	2.5	$0.62^{+0.14}_{-0.16}$	$0.69^{+0.09}_{-0.10}$	$0.58^{+0.17}_{-0.17}$
VAC	2.5	$0.71^{+0.27}_{-0.41}$	$0.39^{+0.55}_{-0.05}$	$0.23^{+0.75}_{-0.02}$

TABLE IV. The normalized ratio,  $N$ , of electron scattering rate to neutrino absorption rate for the 0.862 MeV  ${}^7\text{Be}$  line and for the  ${}^{pep}$  neutrino line. The table entries are the values of  $N$  that are consistent with the four operating solar neutrino experiments at the 95% C.L. Results are presented for different neutrino oscillation scenarios. The definition of  $N$  is given in Eq. (14).

Source	Standard	MSW	MSW	Vacuum
	Electroweak	SMA	LMA	Oscillations
${}^7\text{Be}$	1.0	$15.1^{+34.6}_{-14.0}$	$1.21^{+0.30}_{-0.11}$	$1.13^{+1.70}_{-0.12}$
${}^{pep}$	1.0	$11.7^{+15.2}_{-10.6}$	$1.23^{+0.33}_{-0.14}$	$5.78^{+18.7}_{-4.78}$

TABLE V. For the SMA MSW solution, the table gives the accuracy with which  $N(^7\text{Be})$  and  $N(\text{pep})$  determine neutrino parameters. The entries give the range of  $\sin^2 2\theta$  and  $\Delta m^2$  that are consistent at 95% C.L. with the four operating solar neutrino experiments and for which  $N(^7\text{Be})$  and  $N(\text{pep})$  are predicted by the best-fit SMA solution to be within 20% of the indicated values. The top entry is  $\sin^2 2\theta$  (multiplied by  $10^3$ ) and the lower entry is the difference in the squares of the neutrino masses (multiplied by  $10^6 \text{ eV}^2$ ).

$N(\text{pep}) \setminus N(^7\text{Be})$	1.5	2.0	4.0	6.0	10.0	15.0	20.0	30.0	35.0	40.0	45.0
2.0	3.5 – 6.3	—	—	—	—	—	—	—	—	—	—
	9.8 – 10.3	—	—	—	—	—	—	—	—	—	—
3.0	3.3 – 6.6	3.2 – 7.2	—	—	—	—	—	—	—	—	—
	9.3 – 9.5	8.5 – 9.5	—	—	—	—	—	—	—	—	—
4.5	—	—	3.2 – 8.3	3.3 – 4.4	—	—	—	—	—	—	—
	—	—	7.1 – 7.8	6.8 – 7.1	—	—	—	—	—	—	—
5.8	—	—	3.3 – 8.3	3.3 – 9.1	3.6 – 4.2	—	—	—	—	—	—
	—	—	7.1 – 7.4	6.5 – 7.1	6.0 – 6.3	—	—	—	—	—	—
7.5	—	—	—	4.0 – 9.1	3.6 – 10.0	3.8 – 4.8	4.0 – 4.6	4.4 – 4.8	—	—	—
	—	—	—	6.5 – 6.8	5.9 – 6.3	5.5 – 5.9	5.1 – 5.5	4.8 – 5.0	—	—	—
9.0	—	—	—	—	4.2 – 10.5	4.2 – 10.5	4.2 – 5.5	4.4 – 5.2	4.8 – 5.5	—	—
	—	—	—	—	5.6 – 6.3	5.4 – 5.9	5.1 – 5.5	4.6 – 5.0	4.4 – 4.8	—	—
11.0	—	—	—	—	5.2 – 10.5	4.8 – 11.5	4.8 – 11.5	4.8 – 6.0	4.8 – 6.0	5.0 – 6.0	5.2 – 6.0
	—	—	—	—	5.6 – 5.9	5.1 – 5.8	5.0 – 5.5	4.6 – 5.0	4.4 – 4.8	4.3 – 4.7	4.3 – 4.5
12.0	—	—	—	—	7.2 – 10.5	5.0 – 11.5	5.0 – 11.5	5.0 – 6.6	5.0 – 6.3	5.2 – 6.3	5.2 – 6.3
	—	—	—	—	5.6 – 5.8	5.0 – 5.7	5.0 – 5.5	4.6 – 5.0	4.4 – 4.8	4.2 – 4.7	4.2 – 4.5
18.0	—	—	—	—	—	—	7.6 – 12.0	6.6 – 13.0	6.6 – 13.0	6.6 – 10.5	6.6 – 8.7
	—	—	—	—	—	—	4.6 – 5.0	4.2 – 4.8	4.2 – 4.7	3.9 – 4.6	3.9 – 4.4
24.0	—	—	—	—	—	—	—	8.3 – 12.6	7.9 – 12.6	7.9 – 12.0	7.9 – 12.0
	—	—	—	—	—	—	—	4.0 – 4.4	3.8 – 4.4	3.8 – 4.4	3.9 – 4.3

TABLE VI. For the vacuum oscillation solution, the table gives the accuracy with which  $N(^7\text{Be})$  and  $N(\text{pep})$  determine neutrino parameters. The entries give the range of  $\sin^2 2\theta$  and  $\Delta m^2$  that are consistent at 95% C.L. with the four operating solar neutrino experiments and for which  $N(^7\text{Be})$  and  $N(\text{pep})$  are predicted by the best-fit vacuum oscillation solution to be within 20% of the indicated values. The top entry is  $\sin^2 2\theta$  and the lower entry is the difference in the squares of the neutrino masses (multiplied by  $10^{11} \text{ eV}^2$ ).

$N(\text{pep}) \setminus N(^7\text{Be})$	1.1	1.2	1.4	1.6	2.0	2.5	3.0
1.5	0.67 – 1.0	0.67 – 1.0	0.67 – 1.0	0.67 – 0.98	0.76 – 0.94	0.85 – 0.94	0.89 – 0.92
	5.4 – 10.4	5.4 – 10.5	5.4 – 10.5	6.1 – 10.5	6.2 – 8.0	6.3 – 7.9	6.3 – 6.5
2.0	0.77 – 1.0	0.77 – 1.0	0.77 – 0.98	0.81 – 0.98	0.88 – 0.97	0.92 – 0.94	—
	5.6 – 10.4	5.6 – 10.5	6.0 – 10.6	6.1 – 10.6	6.2 – 10.6	6.29 – 6.31	—
2.5	0.84 – 1.0	0.84 – 1.0	0.85 – 0.98	0.89 – 0.98	0.94 – 0.97	—	—
	5.7 – 8.4	5.7 – 8.4	6.0 – 8.3	6.1 – 6.2	6.2 – 6.2	—	—
3.0	0.89 – 1.0	0.89 – 1.0	0.89 – 0.99	0.92 – 0.99	—	—	—
	5.7 – 8.4	5.7 – 8.4	6.0 – 8.3	6.1 – 6.2	—	—	—
4.0	0.93 – 1.0	0.93 – 1.0	0.93 – 1.0	0.96 – 1.0	—	—	—
	5.8 – 6.1	5.8 – 6.1	6.0 – 6.2	6.1 – 6.2	—	—	—
5.0	0.95 – 1.0	0.95 – 1.0	0.95 – 1.0	0.98 – 1.0	—	—	—
	5.8 – 6.1	5.8 – 6.1	6.0 – 6.15	6.1 – 6.15	—	—	—
10.0	0.98 – 1.0	0.98 – 1.0	0.98 – 1.0	—	—	—	—
	5.9 – 6.1	5.9 – 6.1	6.0 – 6.1	—	—	—	—
15.0	0.99 – 1.0	0.99 – 1.0	0.99 – 1.0	—	—	—	—
	5.9 – 6.0	5.9 – 6.0	6.0 – 6.05	—	—	—	—
20.0	0.996 – 1.0	0.996 – 1.0	1.0 – 1.0	—	—	—	—
	5.9 – 6.0	5.9 – 6.0	6.0 – 6.0	—	—	—	—

## FIGURES

FIG. 1. Recoil Electron Energy Spectrum. The computed recoil electron energy spectrum is shown for different assumed neutrino production and oscillation scenarios. The vertical arrows indicate the maximum electron energy produced by each solar neutrino source. For the standard solar model with no oscillations [24], the spectrum is indicated by a solid line. Assuming the standard model fluxes are modified by neutrino oscillations, the SMA MSW solution is indicated by the dotted lines, the LMA MSW solution by the line with short dashes, and the VAC oscillation solution is indicated by long dashes. The dot-dashed line labeled CNO corresponds to the hypothetical case in which solar energy is derived almost completely by CNO reactions and the neutrino fluxes are modified by a SMA MSW solution [32]. In actual experiments, the sharp features due to individual lines will be made somewhat smoother by finite energy resolution.

FIG. 2. Allowed Parameter Regions for Four Operating Experiments plus New Neutrino-Electron Scattering Experiments. The results shown in the top panel were calculated assuming that the best-fit SMA MSW solution is correct; the middle panel assumes the validity of the LMA solution; and the lowest panel is based upon the vacuum oscillation solution. The regions of  $\Delta m^2$  and  $\sin^2 2\theta$  allowed at 95% C.L. by the four operating experiments are shown by solid lines. Adding a hypothetical measurement of the 0.862 MeV  ${}^7\text{Be}$  neutrino line equal, within an assumed 10% random error, to the value computed using the best-fit neutrino oscillation parameters, the dotted curve shows the allowed regions that would apply for the four operating experiments plus the line measurement. If measurements are made of both the  ${}^7\text{Be}$  and the *pep* neutrino lines, the shaded region applies.

FIG. 3. The predicted solution space for 0.862 MeV  ${}^7\text{Be}$  neutrino-electron scattering rate versus charged current (absorption) rate. The indicated solutions are consistent with the four operating solar neutrino experiments at the 95% C.L. The upper panel shows that the SMA and LMA MSW solutions overlap somewhat in the plane shown, but are well separated from the predictions of the standard solar model, indicated by SSM. The allowed solution space for the vacuum oscillations is displayed in the lower panel. These results illustrate the relation summarized by Eq. (8).

FIG. 4. The predicted solution space for the *pep* neutrino-electron scattering rate versus charged current (absorption) rate. The quantities displayed are the same as in Fig. 3 except that Fig. 4 refers to the *pep* line.

FIG. 5. The Allowed Region in the  $N({}^7\text{Be})$  and  $N(\text{pep})$  plane (see text for an explanation of the notation). The darkened regions are consistent at the 95% C.L. with the four operating solar neutrino experiments. The upper panel shows the allowed solution space for the SMA and LMA MSW solutions and the lower panel shows the allowed solution space for the vacuum oscillations.

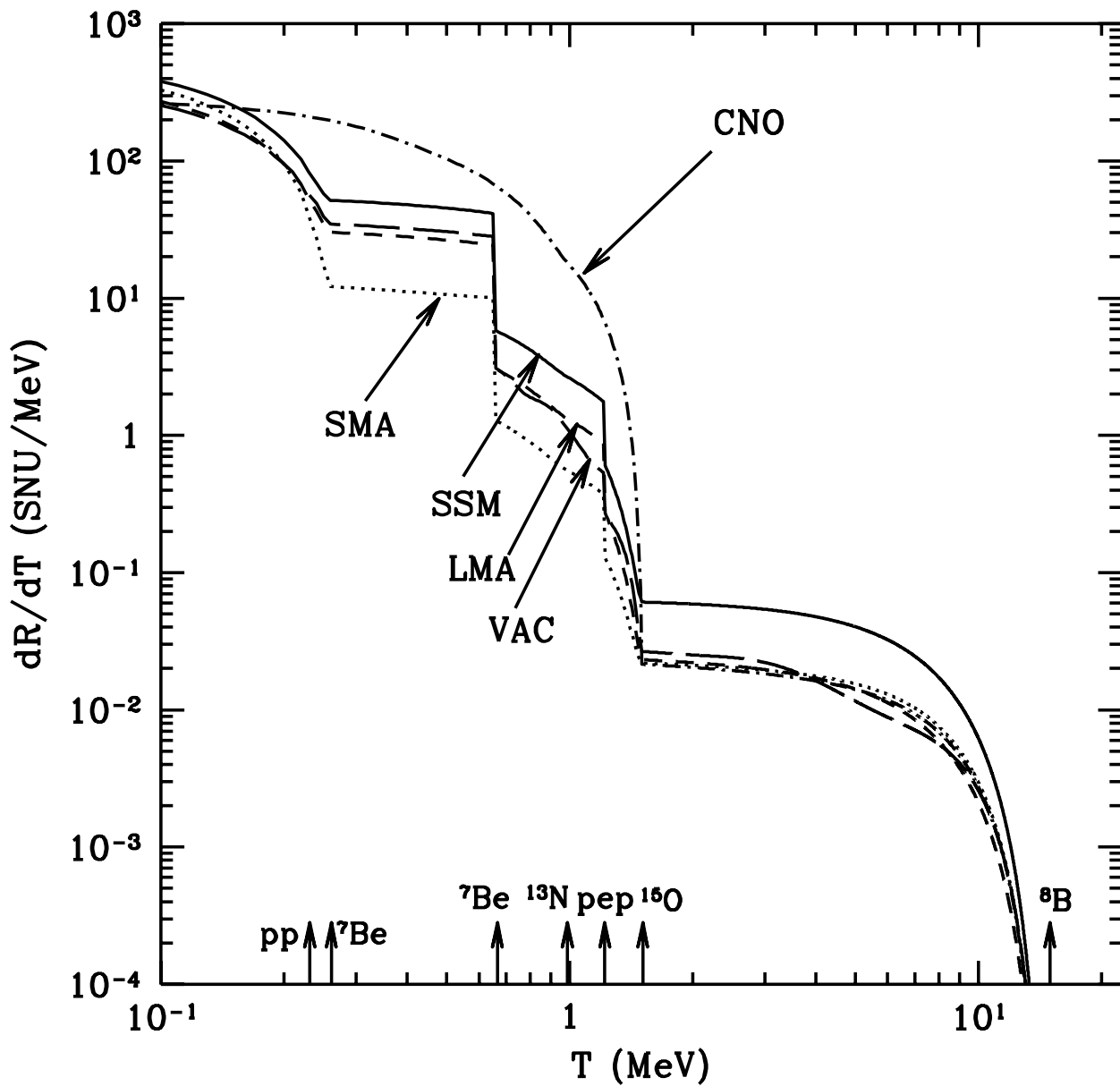


Fig. 1

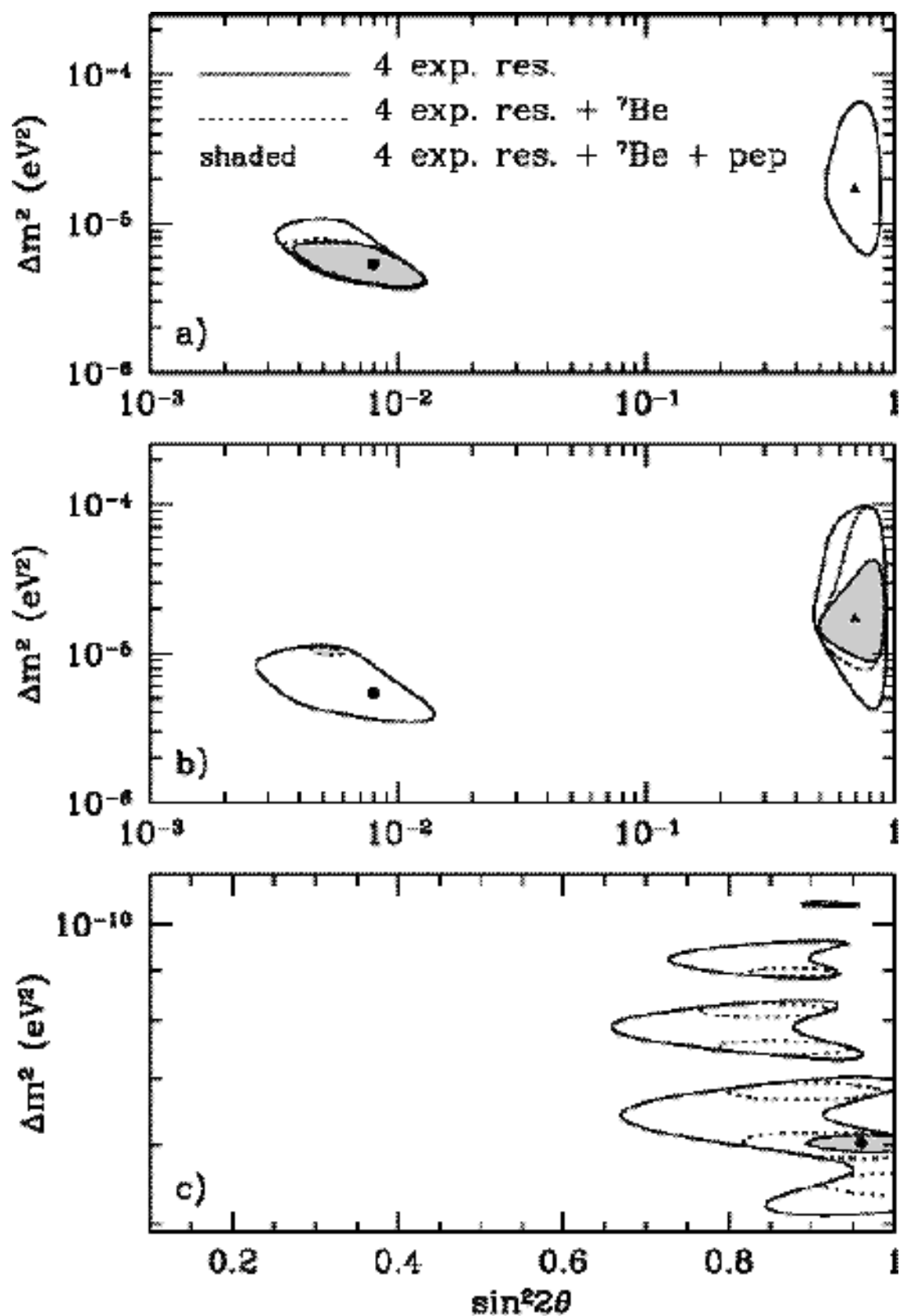


Fig.2

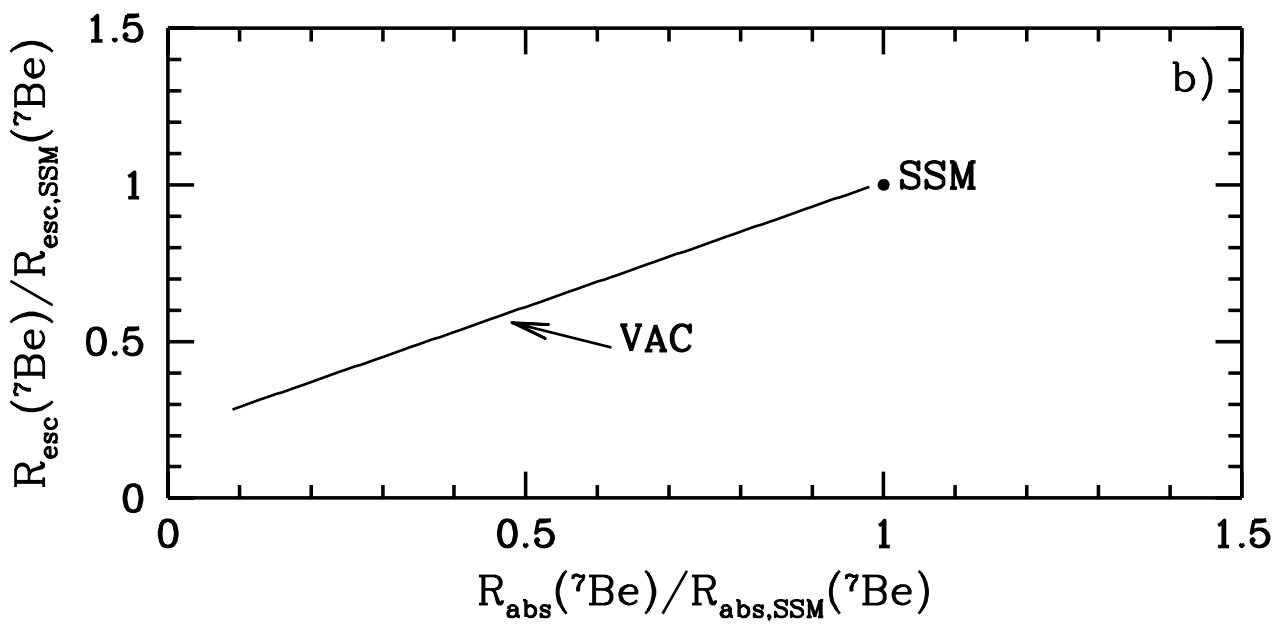
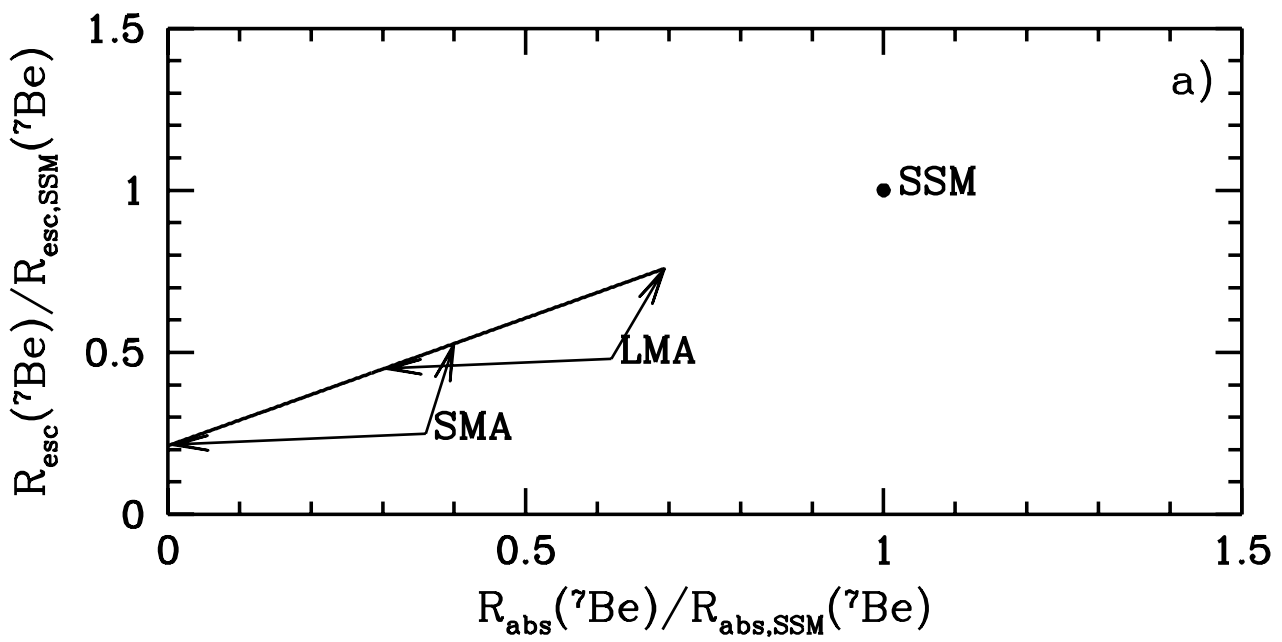


Fig.3

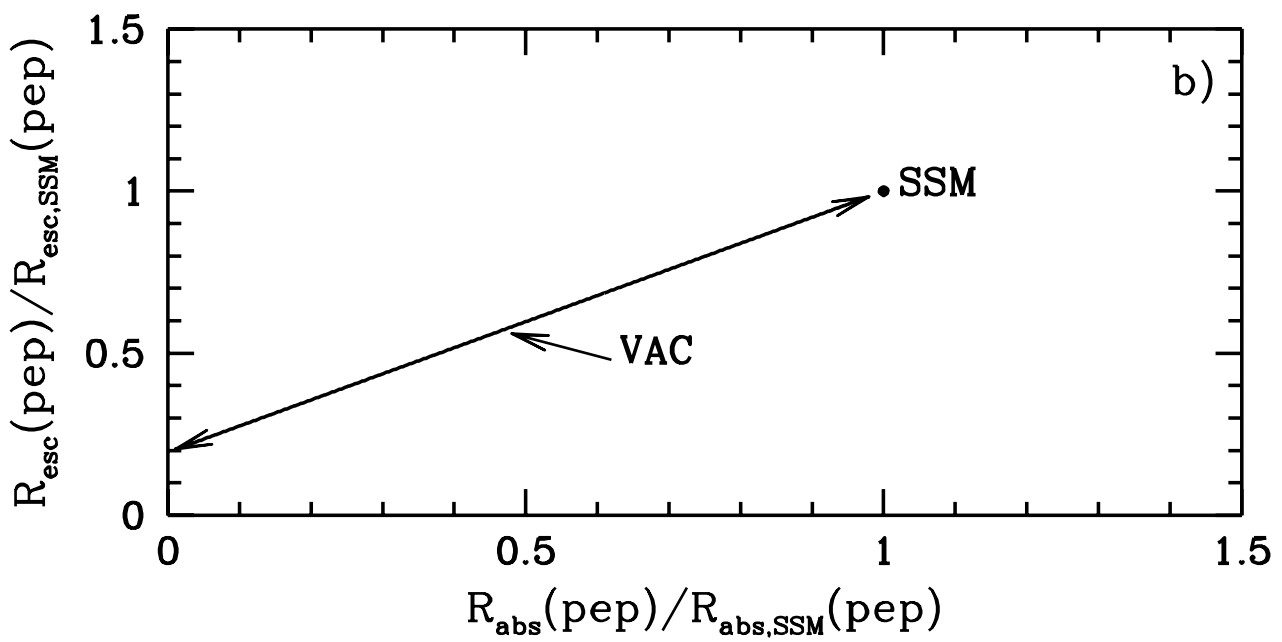
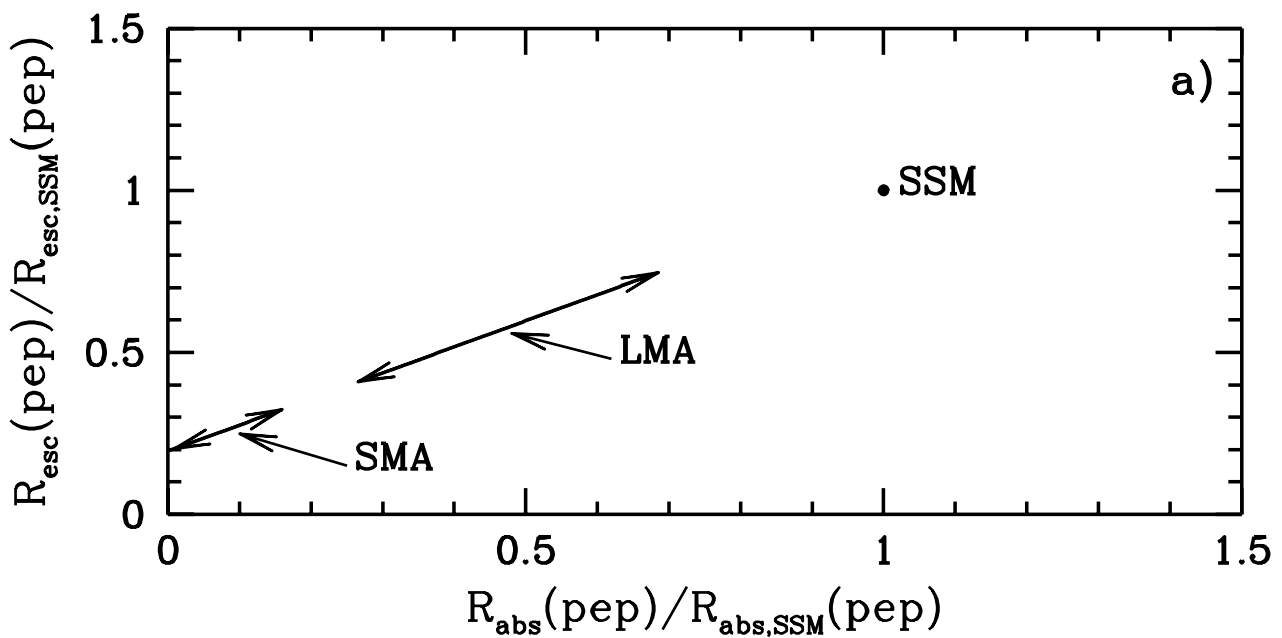


Fig.4

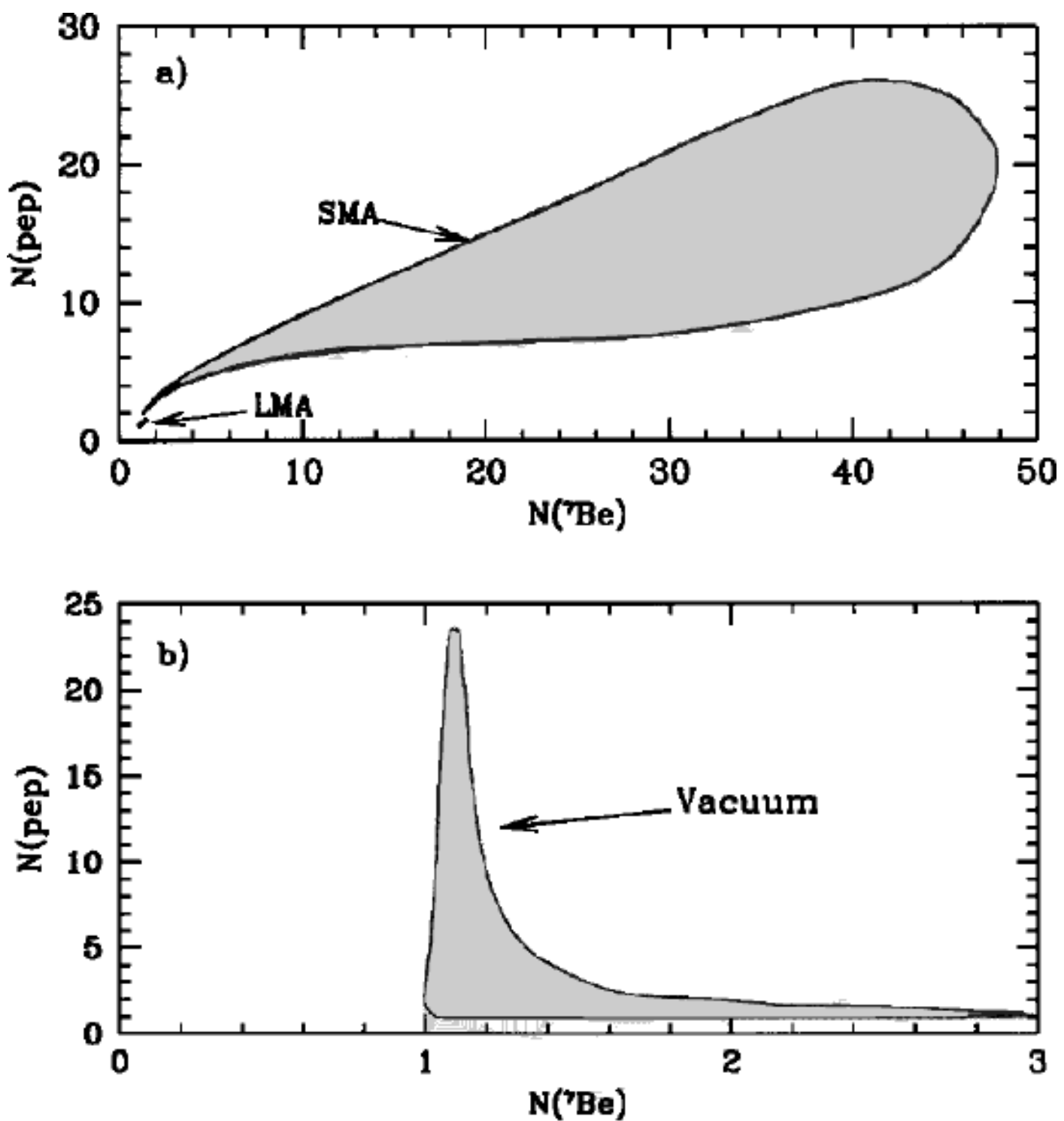


Fig.5